Effect of leaf position and days post-infiltration on transient expression of colorectal cancer vaccine candidate proteins GA733-Fc and GA733-FcK in *Nicotiana benthamiana* plant

5 Kibum Kim[1], Yang Joo Kang[1], Se Ra Park[1], Do-Sun Kim[2], Seung-Won Lee[1], Kinarm Ko[3],
6 Daniel Ponndorf[4], and Kisung Ko[*]

7 [1] Department of Medicine, Therapeutic Protein Engineering Lab, College of Medicine,
8   Chung-Ang University, 84 Heukseok-ro Dongjak-gu, Seoul 156-756, Korea
9 [2] Vegetable Research Division, National Institute of Horticultural and Herbal Science,
10   Rural Development Administration, Wanju-gun, South Korea
11 [3] Department of Stem Cell Biology, Konkuk University School of Medicine, Seoul,
12   Korea
13 [4] Department of Biological Chemistry, John Innes Centre, Norwich Research Park, Colney,
14   Norwich, UK
15 [*] Corresponding Author:
16 Kisung Ko
17 Department of Medicine, Therapeutic Protein Engineering Lab, College of Medicine,
18 Chung-Ang University, 84 Heukseok-ro Dongjak-gu, Seoul 156-756, Korea
19 Email address: ksko@cau.ac.kr

Abstract

21 Immunization with the tumor-associated antigen GA733 glycoprotein, which is highly expressed
22 in colorectal cancer, is considered to be a promising strategy for cancer prevention and treatment.
23 We cloned a fusion gene of GA733 and immunoglobulin Fc fragment (GA733-Fc), and that of
24 GA733-Fc and an endoplasmic reticulum retention motif (GA733-FcK) into the Cowpea mosaic
25 virus (CPMV)-based transient plant expression vector, pEAQ-*HT*. *Agrobacterium tumefaciens*
26 (LBA4404) transformed with the vectors pEAQ-*HT*-GA733-Fc and pEAQ-*HT*-GA733-FcK was
27 infiltrated into the leaves of *Nicotiana benthamiana* plants. To optimize harvesting of leaf to
28 express therapeutic glycoproteins both spatially and temporally, protein expression levels at
29 various leaf positions (top, middle, and base) and days post-infiltration (dpi) were investigated.
30 The GA733-Fc and GA733-FcK genes were detected in leaves at 1–10 dpi using PCR. As
31 assessed by western blot, GA733-Fc and GA733-FcK were expressed at the highest levels in the
32 top leaf position at 5 dpi, and GA733-FcK was expressed more than GA733-Fc. The proteins
33 [GA733-Fc (1.12 mg/g of leaf) and GA733-FcK (11.82 mg/g of leaf)] were successfully purified
34 from infiltrated *N. benthamiana* leaves using protein A affinity chromatography. ELISA verified
35 that an anti-GA733 antibody recognized both purified proteins. Thus, a functional GA733-Fc
36 colorectal cancer vaccine protein can be transiently expressed using a CPMV virus-based vector,
37 with an optimized expression time and leaf position post-infiltration.

38 **Keywords:** Agroinfiltration, fusion protein, KDEL, molecular biopharming, recombinant
39 vaccine

Introduction

40

41   Tumor-associated antigens (TAAs) are promising immunotherapeutic vaccine candidate
42 proteins for cancer prevention and treatment (Lu et al. 2012; Wong-Arce et al. 2017). Immune
43 responses for induction of immunoglobulins to target TAAs have been actively studied (Eun-Wha
44 Son et al. 2005). Among TAAs, glycoprotein GA733, or epithelial cell adhesion molecule
45 (EpCAM), is highly expressed on the surface of colorectal cancer cells and has been extensively
46 investigated (Eyvazi et al. 2018; Lu et al. 2012). Anti-GA733 antibody has been shown to inhibit
47 the growth of colorectal cancer cells, which results from GA733 immunization in mice (Brodzik
48 et al. 2008). The extracellular domain of GA733 is often used as a target for colorectal cancer
49 vaccination and is fused with a human immunoglobulin Fc fragment (GA733-Fc) to enhance
50 immune responses (Kim et al. 2018; Lee et al. 2017). The presence of the Fc domain markedly
51 increases the plasma half-life of the protein, which prolongs therapeutic activity (Czajkowsky et
52 al. 2012), and it simplifies purification of the protein by binding to protein A (Lee et al. 2020; Park
53 et al. 2020).

54   Plants have several advantages over existing mammalian cell-based systems in terms of lower
55 production costs and the absence of human pathogen contamination (Chen et al. 2013; Lee et al.
56 2017; Loh & Wayah 2014; Shin et al. 2019). In addition, plants require a simple cultivation
57 environment (sunlight, water, nutrients, and fertilizer) to grow (Lim et al. 2015; Rigano et al.
58 2005). Moreover, unlike bacterial cells, plants have post-translational modification systems similar
59 to those of mammalian cells, such as glycosylation. Since plant cells are eukaryotic and have an
60 endomembrane system and secretory pathway (Loh & Wayah 2014), plants can produce and
61 assemble correctly folded and complex mammalian proteins in their cells (Menassa et al. 2012;
62 Se-Ra Park 2019). Thus, plants are considered as an attractive alternative for the production of
63 therapeutic recombinant proteins (Lee et al. 2017; Nausch et al. 2012). In our previous study, plants
64 have been determined to highly produce recombinant GA733-Fc fusion proteins (Park et al. 2015).

65   In general, there are two approaches to express recombinant proteins in plants, which are
66 transgenic and transient plant expression (Chen et al. 2013; Joh et al. 2006; Ma et al. 2019; Wydro
67 et al. 2006). For transient expression, the vector pEAQ-*HT*, which is based on the Cowpea mosaic
68 virus (CPMV), has been reported to be an efficient expression vector for therapeutic recombinant
69 proteins (Shah et al. 2013). This deconstructed vector lacks the viral coat protein and has been
70 shown to allow high and fast recombinant protein production (Chen et al. 2013; Daniell et al. 2009;
71 Peyret & Lomonossoff 2013). In addition, *Agrobacterium*-mediated transient expression using a
72 syringe or vacuum machine to transfer the CPMV-based pEAQ vector can be faster, cheaper, and
73 more convenient than traditional stable transformation systems, without the need for viral
74 replication (Loh & Wayah 2014). However, the expression period and plant tissue position can
75 influence both the quality and quantity of the recombinant protein (Lim et al. 2015; Yamamoto et
76 al. 2018).

77   Thus, the goal of our current research is to establish spatial and temporal conditions for the
78 maximum production of the colorectal cancer vaccine candidate proteins GA733-Fc and GA733-
79 Fc with an ER retention motif (GA733-FcK), using the CPMV-based pEAQ transient expression
80 system. In order to study optimal expression of both GA733-Fc and GA733-FcK, the GA733-Fc
81 and GA733-FcK expression vectors were transferred to plant leaves in a laboratory scale using a
82 direct-syringe agroinfiltration method. Gene insertion, protein expression, protein purification, and
83 antibody recognition of both recombinant proteins were investigated along with day post-
84 infiltration and leaf position.

85

Materials & Methods

Plasmid construction

To construct the pEAQ vectors for transient expression of GA733, the sequence encoding the GA733 was ligated to that of human IgG Fc to generate the GA733-Fc fusion gene, and this recombinant gene was tagged with an ER retention signal (KDEL) to generate GA733-FcK (Fig. 1). These sequences were cloned individually into the pEAQ-*HT* vector (Peyret & Lomonossoff 2013; Sainsbury et al. 2009), which is based on CPMV, a non-enveloped plant virus in the Comovirus family consisting of RNA-1 (6.0 kb) and RNA-2 (3.5 kb) molecules (Peyret & Lomonossoff 2013). The T-DNA region of the pEAQ-*HT* vector possesses the suppressor of gene silencing, P19, and the gene encoding neomycin phosphotransferase Ⅲ for resistance to kanamycin (Sainsbury et al. 2009). The GA733-Fc and GA733-FcK sequences were cloned into the AgeI site of pEAQ-*HT* using the In-Fusion® HD Cloning Kit (Takara, Mountain View, CA) (Fig. 1). In the recombinant pEAQ-*HT* vectors, expression of GA733-Fc and GA733-FcK was under the control of the Cauliflower mosaic virus 35S promoter and nopaline synthase terminator (Sainsbury et al. 2009) (Fig. 1). *Agrobacterium tumefaciens* (LBA4404) was transformed with the recombinant binary plasmid vectors, and the resulting transformants were named Ag/pEAQ-GA733-Fc and Ag/pEAQ-GA733-FcK.

Plants for agroinfiltration

N. benthamiana plant was used for agroinfiltration. The seeds of *N. benthamiana* were sown in commercial, nitrogen-fertilized soil (Seoul Bio, Chungcheongbuk-do, Korea). After 14 days, the seedlings were transplanted into pots containing nitrogen-fertilized soil. They were grown in a plant chamber at 25°C with 16 h of light and 8 h of darkness. Water was supplied every 2 days (50–100 ml). The plants were used for experiments after 6 weeks.

Agroinfiltration using the syringe method

Agrobacteria carrying each vector pEAQ-GA733-Fc and pEAQ-GA733-FcK were subcultured on LB agar containing antibiotics (10 μg/ml kanamycin) at 28°C for 48 h. Then, 100 μl of infiltrating medium was inoculated in 40 ml of fresh LB medium with 10 μg/ml kanamycin and incubated for 21–23 h at 28°C with shaking at 210 rpm until 0.35 optical density at 600 nm was obtained. The agrobacteria were pelleted by centrifugation at 3,000 rpm followed by resuspension in 40 ml of MMA buffer (10 mM 2-N-morpholinoethanesulfonic acid, pH 5.6, 10 mM MgCl$_2$, 100 μM acetosyringone) (Sainsbury et al. 2009). The abaxial side of each *N. benthamiana* leaf was pricked using a syringe needle to aid infiltration. Then, MMA buffer containing Ag/pEAQ-GA733-Fc or Ag/pEAQ-GA733-FcK was infiltrated into the undersides of each leaf with soft pressure using a 1 ml syringe (needle removed) until the entire leaf was wet (Loh & Wayah 2014). The plant leaves with the same age were used for agrobacterium inoculation. The same leaf size was used for each location grown during the same period. After infiltration, the plants were grown at 25°C in a chamber and watered every 1–2 days to prevent drying. The infiltrated leaves were harvested as described directly below. All samples were taken in triplicate with the same leaf at the same location for each dpi.

Harvesting agroinfiltrated leaves in accordance with days post-infiltration (dpi)

126   *N. benthamiana* leaf samples were collected at 1, 3, 5, 7, 8, 9, and 10 dpi to determine time-
127   dependent recombinant protein expression levels. The infiltrated top, middle, and base leaves were
128   harvested to investigate spatial protein expression and morphological changes.

129   Protein extraction and western blot analysis

130   The agroinfected leaves were harvested according to leaf positions (top, middle, and base
131   leaves) for western blot analysis. After harvesting, the leaf blades were washed with tap water and
132   gently dried with tissue paper. The harvested leaves (100 mg) were homogenized in three volumes
133   (w/v) of $1\times$ PBS (2.7 mM KCl, 137 mM NaCl, 10 mM Na_2HPO_4 and 2 mM KH_2PO_4) to extract
134   the TSP. Two microliters of each sample was mixed with 0.4 µl of loading buffer (1 M Tris-HCl,
135   10% SDS, 5% 2-mercaptoethanol, 50% glycerol, and 0.1% bromophenol blue) and 16.6 µl of
136   distilled water. The mixed samples were subjected to 10% SDS-PAGE in SDS running buffer (0.2
137   M glycine, 25 mM Tris-HCl, 0.1% [w/v] SDS). The protein gel was transferred to a nitrocellulose
138   membrane (Millipore Corp, Billerica, MA). The blotted membranes were transferred to $1\times$ PBS-
139   T buffer ($1\times$ PBS with 0.5% [v/v] Tween 20) and then blocked in 5% skim milk (Sigma, St. Louis,
140   MO) for 2 h at room temperature. The membrane was incubated with primary mouse anti-EpCAM
141   mAb (anti-GA733 mAb) (R&D Systems, MN) (Isotype IgG_{2a}, 1:5,000 dilution) to detect the
142   GA733 portion of GA733-Fc and GA733-FcK, and then with 1:5,000-diluted secondary HRP-
143   conjugated anti-mouse IgG_{2a} (Abcam, Cambridge, UK), each for 2 h at room temperature with
144   shaking (110 rpm). The protein bands were detected by using SuperSignal Chemiluminescent
145   Substrate (Pierce, Rockford, IL) and visualized by exposure to X-ray film (Fuji, Tokyo, Japan).
146   EpCAM-Fc from mammalian cell (GA733-Fc^M) (rhEpCAM/Fc Chimera, R&D Systems, MN)
147   was used as a positive control, and non-transformed *N. benthamiana* leaves were used as a negative
148   control (Lim et al. 2015).

149   Genomic DNA isolation and PCR

150   Genomic DNA in transfected leaves was isolated using the Genomic DNA Mini Kit
151   (Favorgen, Taiwan), according to the manufacturer's instructions. PCR was conducted to confirm
152   the presence of the GA733-Fc and GA733-FcK genes in the agroinfected leaves using a PCR
153   premix kit (iNtRON Biotechnology, Seoul, Korea). The sequences of the primers were as follows:
154   GA733-Fc forward primer, 5′-CAA ATT CGC GAC CGG ATG GCT ACT CAA CGA AGG-3′
155   and reverse primer, 5′-GGT GAT GCA TAC CGG TCA ACC CGG GGA CAG GGA-3′; GA733-
156   FcK forward primer, 5′-CAA ATT CGC GAC CGG ATG GCT ACT CAA CGA AGG-3′ and
157   reverse primer, 5′-GGT GAT GCA TAC CGG TCA GAG TTC ATC TTT ACC C-3′. The PCR
158   consisted of an initial denaturation at 94°C for 20 min, followed by 30 cycles of denaturation at
159   94°C for 20 s, annealing at 64°C for 30 s, and extension at 72°C for 2 min, and then a final
160   extension at 72°C for 2 min. Non-transfected plants were used as a negative control, while vectors
161   carrying the expression cassettes of GA733-Fc and GA733-FcK in *Escherichia coli* were used as
162   positive controls.

163   Purification of GA733-IgG Fc and GA733-IgG FcK proteins from agroinfected leaves

164   To purify GA733-Fc and GA733-FcK, 100 g of agroinfected leaves were homogenized in
165   extraction buffer (37.5 mM Tris-HCl, pH 7.5, 50 mM NaCl, 15 mM EDTA pH 8.0, 75 mM sodium
166   citrate, and 0.2% sodium thiosulfate) using an aluminum blender (Hanil, Seoul, Korea) and then
167   centrifuged at 7,000 $\times$ *g* for 30 min at 4°C. The supernatant was collected, further clarified using
168   Miracloth (Biosciences, La Jolla, CA), and adjusted to pH 5.1 with acetic acid. The protein solution

169   was then centrifuged at 10,000 × *g* for 30 min. The supernatant was collected, further clarified
170   using Miracloth, and adjusted to pH 7.0 with 3 M Tris-HCl. Eight percent of the total supernatant
171   volume of ammonium sulfate was added to the supernatant, and the solution was incubated at 4°C
172   for 2 h, and then 22.6% ammonium sulfate was added to the total solution volume. The mixture
173   was incubated overnight at 4°C and then centrifuged at 8,000 × *g* for 30 min at 4°C. The pellet
174   was resuspended in 1/10 of the original volume of extraction buffer, and then centrifuged again at
175   8000 × *g* for 30 min at 4°C. The supernatant was filtered through a 0.45-μm syringe filter
176   (MILLEX, Germany) and loaded on a protein A resin column (Sepharose 4 Fast Flow, GE
177   Healthcare, Sweden, NJ). The target proteins were eluted using elution buffer according to the
178   manufacturer's recommendations. The final eluted protein fractions were subjected to SDS-PAGE
179   to assess their purity. The gel was stained with Coomassie blue staining solution [10% acetic acid
180   (v/v), 30% methanol (v/v), and 0.01% Coomassie blue (w/v)] at room temperature for 30 min with
181   shaking. The gel was destained with destaining solution (10% acetic acid and 30% methanol) thrice
182   for 30 min each with shaking. The stock GA733-Fc and GA733-FcK protein solutions were
183   dialyzed three times against sterile 1× PBS.

184   ELISA to confirm the ability of GA733-Fc and GA733-FcK to bind anti-GA733 antibody

185   MaxiSorp™ 96-well ELISA plates (Nunc, Rochester, NY) were coated with 100 μl per well
186   of carbonate-bicarbonate (Sigma-Aldrich, St. Louis, MO) buffer containing mouse anti-EpCAM
187   mAb (anti-GA733 mAb) (R&D Systems, MN) (50 ng) and were incubated overnight at 4°C. The
188   plates were washed four times with 1× PBS-T [1× PBS plus 0.5% (v/v) Tween 20]. After washing,
189   serially diluted GA733-Fc and GA733-FcK protein samples (12.5 ng to 0.196 ng) were added to
190   each well, and then the plates were incubated for 2 h at 37°C. The wells were washed four times
191   with 1× PBS-T. One hundred microliters of HRP-conjugated goat anti-human IgG Fc antibody
192   (Jackson, West Grove, PA; diluted 1:5,000) was added to each well as a secondary antibody. After
193   incubating for 2 h at room temperature, 3,3′,5,5′-tetramethylbenzidine (TMB) substrate solution
194   (Seracare, Milford, MA) was added to each well, and the color was allowed to develop for 3 min.
195   TMB Stop Solution (Seracare, Milford, MA) was used to stop the reaction. The absorbance of each
196   well was read at 450 nm on a Gen5 microplate reader with version 2.01 software (Biotek,
197   Winooski, VT).
198

199   **Results**

200   Morphological changes in top, middle, and base leaves after agroinfiltration

201   To investigate morphological changes in the plant leaves after agroinfiltration, the leaf
202   morphology of *N. benthamiana* plants agroinfiltrated with *Agrobacterium* carrying pEAQ-GA733-
203   Fc (Ag/pEAQ-GA733-Fc) and Ag/pEAQ-GA733-FcK was examined according to days post-
204   infiltration (dpi) and leaf position (top, middle, and base) (Fig. 2). In plants agroinfiltrated with
205   Ag/pEAQ-GA733-Fc, leaf chlorosis was not observed (top, middle, and base leaves) until 3 dpi
206   (Fig. 2A). The base leaves started to show chlorosis at 5 dpi. The middle and top leaves showed
207   chlorosis at 7 dpi (Fig. 2A). Serious necrosis was observed on the base leaves at 8 dpi, while
208   necrosis was observed on the middle and top leaves at 9 and 10 dpi, respectively. In plants
209   agroinfiltrated with Ag/pEAQ-GA733-Fc and Ag/pEAQ-GA733-FcK, chlorosis and necrosis
210   began on the base leaves at 5 and 7 dpi, respectively (Fig. 2B). The middle and top leaves both
211   showed chlorosis and necrosis at 7 and 8 dpi, which was 2–3 days later than the base leaves (Fig.

212 2B). At 10 dpi, all the base leaves agroinfiltrated with both vectors showed necrosis (Fig. 2). After
213 7 dpi, regardless of the transgene, all the base leaves showed chlorosis and necrosis with wilting,
214 and the leaf mass decreased rapidly (Fig. 2).

215 PCR confirmation of GA733-Fc and GA733-FcK genes in agroinfiltrated leaves of *N.*
216 *benthamiana*

217 PCR analysis was conducted to confirm the presence of the genes encoding GA733-Fc and
218 GA733-FcK in the agroinfiltrated leaves at each leaf position (top, middle, and base leaves) (Fig.
219 3). The expected sizes of the amplified GA733-Fc (1,461 bp) and GA733-FcK (1,473 bp) bands
220 were observed regardless of leaf position (Fig. 3). There was no band in the genomic DNA sample
221 from a plant not infiltrated with *Agrobacterium* (Fig. 3). In plants agroinfiltrated with Ag/pEAQ-
222 GA733-Fc, the top and middle leaves produced PCR bands at all observed dpi (Fig. 3A). All the
223 base leaves at 1, 3, 5, and 7 dpi produced the PCR band. In plants agroinfiltrated with Ag/pEAQ-
224 GA733-FcK, the PCR band trends were similar to those with Ag/pEAQ-GA733-Fc (Fig. 3B). The
225 agroinfiltrated base leaves at 8, 9, and 10 dpi were not included for PCR analysis owing to the lack
226 of sample mass caused by severe chlorosis, necrosis, and wilting.

227 Western blot analysis to determine the expression levels of GA733-Fc and GA733-FcK
228 according to leaf position

229 Western blot analysis was performed to investigate the differences in expression levels of
230 GA733-Fc and GA733-FcK depending on the leaf position (top, middle, and base leaves) and dpi
231 (Fig. 4). To compare the protein expression level, 2 μl of each sample extracted from equal
232 biomasses was loaded in each western blot lane. In GA733-Fc, there were a 65 kDa and >240 kDa
233 protein bands for the top leaves at 3, 5, and 7 dpi. At 5 dpi, the 65 kDa band density was the
234 strongest among the others in the leaves agroinfiltrated with Ag/pEAQ-GA733-Fc (Fig. 4A left
235 panels). In the middle and base leaves, the 65 kDa band was not detected. However, in the middle
236 leaves at 3–10 dpi, several bands larger than 240 kDa were detected. In plants agroinfiltrated with
237 Ag/pEAQ-GA733-FcK, there were 65 and ~240 kDa protein bands for the top leaves at all dpi
238 (Fig. 4A right panel). The middle leaves also showed the ~65 and ~240 kDa protein bands at 5, 7,
239 8, and 9 dpi, whereas at 3 and 10 dpi, the bands were barely detected (Fig. 4A right middle). In the
240 base leaves, only the ~240 kDa protein band was detected at 8 dpi. In general, protein expression
241 was higher for GA733-FcK than for GA733-Fc (Fig. 4B). The top leaf position showed relatively
242 high expression regardless of the vector type (Fig. 4B). There was almost no protein expression in
243 the base leaf position (Fig. 4). From the highest to the lowest, the relative protein density levels
244 were ranked top, middle, and base. In general, the highest band density was observed at 5 dpi in
245 the top leaves (Fig. 4).

246 Purification of GA733-Fc and GA733-FcK from agroinfected N. benthamiana plant leaves

247 GA733-Fc and GA733-FcK transiently expressed in *N. benthamiana* leaves were purified
248 (Fig. 5). The SDS-PAGE analysis showed that the GA733-Fc and GA733-FcK proteins were
249 successfully purified using protein A affinity chromatography (Fig. 5). Monomer protein bands of
250 the expected size (~65 kDa) were detected for both plant-derived GA733-Fc (GA733-Fc^P) and
251 GA733-FcK^P. The dimeric protein band (~140 kDa) was also observed in the purified GA733-
252 FcK^P. The protein band intensity was stronger for GA733-FcK than for GA733-Fc (Fig. 5). Indeed,
253 1.12 mg of GA733-Fc and 11.82 mg of GA733-FcK were purified from 100 g of infiltrated N.
254 *benthamiana* leaves (5 dpi).

255 ELISA to confirm binding of GA733-Fc^P and GA733-FcK^P proteins to anti-GA733 antibody

256   ELISA was conducted to compare the binding of GA733-Fc^P and GA733-FcK^P to an anti-
257 GA733 antibody. The 96-well plate was coated with anti-EpCAM antibody (anti-GA733) (50
258 ng/well), and the purified GA733-Fc^P and GA733-FcK^P proteins were applied (Fig. 6B). Anti-
259 human IgG Fc antibody conjugated to horseradish peroxidase (HRP) was used as a secondary
260 antibody to bind the Fc region of both GA733-Fc^P and GA733-FcK^P (Fig. 6B). The signal from
261 GA733-Fc^P and GA733-FcK^P was higher than that from EpCAM-Fc^M. The GA733-FcK^P showed
262 a higher absorbance compared to the GA733-Fc^P (Fig. 6).

263

Discussion

265   We demonstrated that the leaf tissue position and days post-infiltration (dpi) affected the
266 transient expression level of recombinant GA733 protein fused to an human immunoglobulin Fc
267 fragment (GA733-Fc) and GA733-Fc fused to an ER retention motif (GA733-FcK) in *N.*
268 *benthamiana* plant. For transgenic plant expression, a transformation strategy is required to stably
269 integrate the gene of interest into the plant genome. This transgenic approach has some advantages
270 in terms of scaling up production since the transgene is stably inherited through generations and
271 transgenic seeds can be stored for large-scale cultivation (Chen et al. 2013; Daniell et al. 2009;
272 Peyret & Lomonossoff 2013). However, it has some disadvantages; for instance, generating plant
273 lines requires a long time with low yields of the target protein. On the contrary, plant transient
274 expression system can overcome these drawbacks of time and yield. For transient expression, plant
275 viral or non-viral vectors are utilized to express genes of interest in plants (Chen et al. 2013).
276 Among these strategies, deconstructed viruses that lack the viral coat protein gene allow for
277 production of heterologous proteins in a few days (Alamillo et al. 2006; Chen et al. 2013; Peyret
278 & Lomonossoff 2013). Elimination of the region encoding the coat protein enhances the transgene
279 capacity of the virus, enabling it to efficiently produce large recombinant proteins (Chen et al.
280 2013). In addition, the deconstructed virus vector can replicate in plant cells to a higher level than
281 the full-virus system, allowing a larger amount of recombinant protein to be harvested (Chen et al.
282 2013).
283   In the present study, we hypothesized that the transient protein expression levels of GA733-
284 Fc and GA733-FcK varied depending on the leaf position (top, middle, and base) and transfection
285 periods. Thus, the ultimate goal of this study was to optimize the leaf position for agroinfiltration
286 and leaf harvesting time to enhance production of GA733-Fc and GA733-FcK using the plant
287 transient expression system. First, the morphological changes in the leaves (top, middle, and base)
288 at the dpi were investigated. According to the data, 5–7 dpi was the best time for leaf harvesting
289 and purification of recombinant protein since the leaves during these days showed the least damage
290 (i.e., chlorosis, necrosis, and wilting), and the area of the leaves did not reduce when compared to
291 those on the other later days. The loss of chloroplasts results in loss of energy-generating capacity
292 and reduced protein production capacity (Munné-Bosch & Alegre 2002). Thus, the chlorosis,
293 necrosis, and wilting of leaves induced by *Agrobacterium* infiltration might affect production of
294 the recombinant protein.
295   To confirm GA733-Fc and GA733-FcK gene insertion, PCR analysis was conducted. The
296 expected sizes of the amplified PCR bands were observed (GA733-Fc: 1,461 bp, GA733-FcK:
297 1,473 bp). However, the base leaves of both GA733-Fc and GA733-FcK plants at 8, 9, and 10 dpi
298 were not included in the analysis since the sample mass was insufficient for PCR analysis owing

299 to chlorosis, necrosis, and wilting. All the tested leaf samples produced the expected PCR products,
300 indicating that the infiltration properly delivered both the GA733-Fc and GA733-FcK gene
301 expression cassettes. However, the presence of the transgene in the leaf does not necessarily mean
302 expression of the GA733-Fc and GA733-FcK proteins. Thus, western blotting was carried out to
303 confirm their protein expression. The band of mammalian-derived GA733-Fc was slightly
304 different from plant-derived GA733-Fc and GA733-FcK. It is speculated that the discrepancy is
305 due to difference between mammalian and plant glycosylation, which affects molecular weight,
306 altering protein migration on a western blot (Unal et al. 2008). Accordingly, the protein expression
307 of GA733-Fc and GA733-FcK increased until 5 dpi in the top and middle leaves and then
308 decreased, while the protein expression level in the base leaves was relatively low. In the leaves
309 infiltrated with *Agrobacterium* carrying the GA733-Fc expression vector, the GA733-Fc protein
310 (~65 kDa) was detected in the upper leaves only at 3, 4, and 5 dpi. The fluctuation of protein
311 expression of GA733-FcK is due to the extreme transient expression of foreign proteins localized
312 in ER during 5~7 dpi resulting in temporary plant cell stress such as ER stress (Howel 2013) or
313 temporary protease expression and activation (Mandal et al. 2016). In addition, the western blot
314 analysis showed that the protein expression level was higher in the leaves infiltrated with
315 *Agrobacterium* carrying the GA733-FcK expression vector than in the leaves infiltrated with the
316 GA733-Fc expression vector. These results indicate that the KDEL ER retention signal affected
317 the production level of the GA733-Fc fusion protein in the transient plant expression system. In
318 previous studies, KDEL tagging to recombinant antibodies and antigens localized and accumulated
319 them in the ER, eventually increasing their production levels in transgenic plants (Kang et al. 2016;
320 Lee et al. 2013; Lee et al. 2020; Park et al. 2020; So et al. 2013; Song et al. 2018). Indeed, *N*-
321 glycosylation analysis showed that GA733-FcK had mainly oligo-mannose compared to GA733-
322 Fc, indicating the KDEL induced ER retention of GA733-FcK (Fig. S1).
323   Both GA733-Fc and GA733-FcK expression levels in the leaves decreased in the order of top,
324 middle, and base. The bottom leaves become the main leaves first after germination. These leaves
325 are older with fewer chloroplasts, resulting in lower energy and protein production than the middle
326 and top leaves, which are younger (Munné-Bosch & Alegre 2002). Such low recombinant protein
327 expression is probably related to the low concentration of total soluble protein in the old leaves
328 (Halfhill et al. 2003).
329   For purification of both GA733-Fc and GA733-FcK, protein A affinity chromatography was
330 utilized since the Fc domain was fused to the GA733 protein (Lee et al. 2020; Park et al. 2015;
331 Park et al. 2020; Shin et al. 2019). SDS-PAGE showed that the purified GA733-FcK had stronger
332 band intensity than the purified GA733-Fc. The concentration of the purified GA733-Fc and
333 GA733-FcK proteins was 0.112 and 1.82 mg/ml, respectively, representing 16.25 times higher
334 production of GA733-FcK than GA733-Fc. The enhanced protein production of GA733-FcK in
335 the current study is consistent with that in a previous study, where the transient expression of ER-
336 targeted human interleukin-6 represented 7% of the total soluble protein (TSP) in *N. benthamiana*
337 (Munné-Bosch & Alegre 2002). We speculate that the ER-retained GA733-Fc protein molecules
338 interacted with ER-resident chaperones to promote correct folding (Benchabane et al. 2008) and
339 were less exposed to proteases in the ER (Vitale & Pedrazzini 2005) in transient plant system.
340   In this present study, we confirmed that the protein expression varied with the dpi. After
341 agroinfiltration of the GA733-FcK vector, the top leaves began to express the protein at 3 dpi, with
342 strong expression from 5 to 9 dpi, except for 7 dpi. For the middle leaves, the highest expression
343 was observed at 5 dpi. These results suggest that the best leaf harvesting time for purification of
344 GA733-FcK proteins is 5 dpi and that GA733-Fc can be transiently expressed using the CPMV

345 virus-based vector with an optimized transfection period and leaf position. According to the
346 current results, this harvesting time is applicable for top leaves infiltrated with *Agrobacterium*
347 carrying the GA733-Fc vector. Previous studies also showed high expression of recombinant
348 proteins at 4–6 dpi (Norkunas et al. 2018). The leaf tissue position and dpi affect both GA733-Fc
349 and GA733-FcK recombinant protein expression. Thus, to optimize protein expression, the top
350 leaves should be infiltrated and then harvested from 5 to 9 dpi, and not before 3 dpi and after 9
351 dpi.
352   Sandwich ELISA was performed to detect the binding of each purified GA733-Fc and GA733-
353 FcK protein to an anti-GA733 antibody. The resulting absorbance of GA733-FcK was stronger
354 than that of GA733-Fc. These results suggest that the antibody is able to bind GA733-FcK better
355 than GA733-Fc, and they are similar to our previous studies where recombinant proteins tagged
356 with KDEL showed better interactions with antibodies regardless of the specific antigen or
357 antibody (Kang et al. 2016; Lee et al. 2013; So et al. 2013; Song et al. 2018). We speculate that
358 ER-retained recombinant proteins are more likely to be correctly folded or favorably glycosylated
359 for better binding activity than cytosolic or apoplastic proteins. In the surface plasmon resonance
360 (SPR) analysis (Fig. S2), in addition, GA733-FcK had higher affinity for FcγR I (CD64) than
361 GA733-Fc, indicating that the Fc domain of GA733-FcK interacts better with FcγR I (CD64) than
362 that of GA733-Fc.
363

Conclusions

365
366 In this study, we determined the optimal leaf position and dpi for the transient expression of
367 GA733-Fc and GA733-FcK. In addition, we confirmed that KDEL tagging of GA733-Fc enhanced
368 its production in the transient plant expression system. Taken together, the Fc fusion protein
369 GA733-Fc can be expressed using a CPMV virus-based vector in transient plant system. Plants
370 are in the spotlight as an excellent therapeutic protein production platform. We have expressed and
371 purified colorectal cancer vaccine recombinant protein GA733-Fc and GA733-Fc with KDEL
372 (GA733-FcK) by transient expression system using pEAQ-HT vector with reduced labor than
373 transgenic expression system. By using our currently described optimized GA733-Fc and GA733-
374 FcK transient expression condition, it is expected that mass production of GA733-Fc and GA733-
375 FcK would be realized in the future.
376

Acknowledgements

378 We thank Professor George Lomonossoff (John Innes Centre, Norwich, United Kingdom) for
379 providing the plant viral pEAQ-*HT* vector. This study was conducted in Department of Medicine,
380 Therapeutic Protein Engineering Lab, College of Medicine, Chung-Ang University.

381

References

383 Alamillo JM, Monger W, Sola I, García B, Perrin Y, Bestagno M, Burrone OR, Sabella P,
384   Plana-Durán J, and Enjuanes L *Biotechnology journal*. 2006. Use of virus vectors for the
385   expression in plants of active full-length and single chain anti-coronavirus antibodies.
386   1:1103-1111.

387 Benchabane M, Goulet C, Rivard D, Faye L, Gomord V, and Michaud D *Plant biotechnology*
388   *journal*. 2008. Preventing unintended proteolysis in plant protein biofactories. 6:633-648.
389 Brodzik R, Spitsin S, Golovkin M, Bandurska K, Portocarrero C, Okulicz M, Steplewski Z, and
390   Koprowski H *Cancer Immunol Immunother*. 2008. Plant-derived EpCAM antigen induces
391   protective anti-cancer response.   57:317-323.
392 Chen Q, Lai H, Hurtado J, Stahnke J, Leuzinger K, Dent M *NIH Public Access*. 2013.
393   Agroinfiltration as an effective and scalable strategy of gene delivery for production of
394   pharmaceutical proteins.   1.
395 Czajkowsky DM, Hu J, Shao Z, and Pleass RJ *EMBO Molecular Medicine*. 2012. Fc-fusion
396   proteins: new developments and future perspectives.   4:1015-1028.
397 Daniell H, Singh ND, Mason H, and Streatfield SJ *Trends in Plant Science*. 2009. Plant-made
398   vaccine antigens and biopharmaceuticals.   14:669-679.
399 Eun-Wha Son, Sang-Whan In, and Suhkneung Pyo *Immune Network*. 2005. Cancer Vaccines.
400   5:55-67.
401 Ersin Selcuk Unal, Roongbao Zhao, Andong Qui, and I. David Goldman *Biochim Biophys Acta*
402   *Biomembr*. 2008. N-linked glycosylation and its impact on the electtrophoretic mobility
403   and function of the human proton-coupled folate transporter (*Hs*PCFT). 1407-1414.
404 Eyvazi S, Farajnia S, Dastmalchi S, Kanipour F, Zarredar H, and Bandehpour M *Current Cancer*
405   *Drug Targets*. 2018. Antibody based EpCAM targeted therapy of cancer, review and
406   update.   18:857-868.
407 Halfhill M, Millwood R, Weissinger A, Warwick S, Stewart C *Theoretical and Applied Genetics*.
408   2003. Additive transgene expression and genetic introgression in multiple green-
409   fluorescent protein transgenic crop× weed hybrid generations.   107:1533-1540.
410 Joh LD, McDonald KA, and VanderGheynst JS *Biotechnology Progress*. 2006. Evaluating
411   extraction and storage of a recombinant protein produced in agroinfiltrated lettuce.
412   22:723-730.
413 Kang Y, Shin YK, Park S-W, Ko K *Horticulture, Environment, and Biotechnology*. 2016. Effect
414   of nitrogen deficiency on recombinant protein production and dimerization and growth in
415   transgenic plants.   57:299-307.
416 Kim D-S, Song I, Ko K *Horticulture, Environment, and Biotechnology*. 2018. Low risk of pollen-
417   mediated gene flow in transgenic plants under greenhouse conditions.   59:723-728.
418 Lee J-H, Park D-Y, Lee K-J, Kim Y-K, So Y-K, Ryu J-S, Oh S-H, Han Y-S, Ko K, and Choo Y-
419   K *Plos One*. 2013. Intracellular reprogramming of expression, glycosylation, and function
420   of a plant-derived antiviral therapeutic monoclonal antibody.   8.
421 Lee JH, Ko K *Biomolecules & Therapeutics*, and therapeutics. 2017. Production of recombinant
422   anti-cancer vaccines in plants.   25:345.
423 Lee JH, Park SR, Phoolcharoen W, and Ko K *Plant Biotechnology Reports*. 2020. Expression,
424   function, and glycosylation of anti-colorectal cancer large single-chain antibody (LSC) in
425   plant.1-9.
426 Lim C-Y, Lee KJ, Oh D-B, and Ko K *Frontiers in Plant Science*. 2015. Effect of the developmental
427   stage and tissue position on the expression and glycosylation of recombinant glycoprotein
428   GA733-FcK in transgenic plants.   5:778.
429 Loh H-S, and Wayah S *Asian Journal of Biotechnology*. 2014. Optimizations of laboratoryscale
430   vacuum-assisted agroinfiltration for delivery of a transgene in Nicotiana benthamiana.
431   6:1-14.

432 Lu Z, Lee K-J, Shao Y, Lee J-H, So Y, Choo Y-K, Oh D-B, Hwang K-A, Oh SH, and Han YS
433   *BioMed Research International*. 2012. Expression of GA733-Fc fusion protein as a vaccine
434   candidate for colorectal cancer in transgenic plants.   2012.
435 Ma T, Li ZY, and Wang S *Frontiers in Plant Science*. 2019. Production of Bioactive Recombinant
436   rPA (Reteplase) by Virus-based Transient Expression System in Nicotiana benthamiana.
437   10:1225.
438 Menassa R, Ahmad A, and Joensuu JJ *Molecular farming in plants: recent advances and future*
439   *prospects*: Springer. 2012. Transient expression using agroinfiltration and its applications
440   in molecular farming. 183-198.
441 Munné-Bosch S, and Alegre L *Planta*. 2002. Plant aging increases oxidative stress in chloroplasts.
442   214:608-615.
443 Nausch H, Mikschofsky H, Koslowski R, Meyer U, Broer I, and Huckauf J *Plos One*. 2012. High-
444   level transient expression of ER-targeted human interleukin 6 in Nicotiana benthamiana.
445   7.
446 Norkunas K, Harding R, Dale J, and Dugdale B *Plant Methods*. 2018. Improving agroinfiltration-
447   based transient gene expression in Nicotiana benthamiana.   14:1-14.
448 Park SR, Lim C-Y, Kim D-S, and Ko K *Frontiers in Plant Science*. 2015. Optimization of
449   ammonium sulfate concentration for purification of colorectal cancer vaccine candidate
450   recombinant protein GA733-FcK isolated from plants.   6:1040.
451 Park SR, Lee J-H, Kim K, Kim TM, Lee SH, Choo Y-K, Kim KS, and Ko K *International Journal*
452   *of Molecular Sciences*. 2020. Expression and In Vitro Function of Anti-Breast Cancer
453   Llama-Based Single Domain Antibody VHH Expressed in Tobacco Plants.   21:1354.
454 Peyret H, and Lomonossoff GP *Plant Molecular Biology*. 2013. The pEAQ vector series: the easy
455   and quick way to produce recombinant proteins in plants.   83:51-58.
456 Rigano MM, Walmsley AM *Immunology and Cell Biology*. 2005. Expression systems and
457   developments in plant-made vaccines.   83:271-277.
458 Sainsbury F, Thuenemann EC, and Lomonossoff GP *Plant Biotechnology Journal*. 2009. pEAQ:
459   versatile expression vectors for easy and quick transient expression of heterologous
460   proteins in plants.   7:682-693.
461 Se-Ra Park. 2019. Expression and functional analysis of immunotherapeutic recombinant proteins
462   in heterologous host systems. The Graduate School Chung-Ang University.
463 Shah KH, Almaghrabi B, and Bohlmann H *Plant Molecular Biology Reporter*. 2013. Comparison
464   of expression vectors for transient expression of recombinant proteins in plants.   31:1529-
465   1538.
466 Shin C, Kang Y, Kim H-S, Shin YK, Ko K *Animal Cells and Systems*. 2019. Immune response of
467   heterologous recombinant antigenic protein of viral hemorrhagic septicemia virus (VHSV)
468   in mice.   23:97-105.
469 So Y, Lee K-J, Kim D-S, Lee J-H, Oh D-B, Hwang K-A, Ko K, Choo Y-K, Ko K *Plant Cell,*
470   *Tissue and Organ Culture*. 2013. Glycomodification and characterization of anti-colorectal
471   cancer immunotherapeutic monoclonal antibodies in transgenic tobacco.   113:41-49.
472 Song I, Kang Y, Lee YK, Myung S-C, and Ko K *Plos One*. 2018. Endoplasmic reticulum retention
473   motif fused to recombinant anti-cancer monoclonal antibody (mAb) CO17-1A affects mAb
474   expression and plant stress response.   13.
475 Stephen H. Howell *Annual Review of Plant Biology*. 2016. Endoplasmic reticulum stress responses
476   in plants. 64:477-499

477   Vitale A, and Pedrazzini E *Molecular Interventions*. 2005. Recombinant pharmaceuticals from
478   plants: the plant endomembrane system as bioreactor.   5:216.
479   Wong-Arce A, González-Ortega O, and Rosales-Mendoza S *Trends in Biotechnology*. 2017. Plant-
480   made vaccines in the fight against cancer.   35:241-256.
481   Wydro M, Kozubek E, and Lehmann P *The Journal of the Polish Biochemical Society and of the*
482   *Polish Academy of Sciences*. 2006. Optimization of transient Agrobacterium-mediated
483   gene expression system in leaves of Nicotiana benthamiana.   53:289-298.
484   Yamamoto T, Hoshikawa K, Ezura K, Okazawa R, Fujita S, Takaoka M, Mason HS, Ezura H, and
485   Miura K *Scientific Reports*. 2018. Improvement of the transient expression system for
486   production of recombinant proteins in plants.   8:1-10.
487

Legends of figure

489   **Figure 1.** Schematic diagram of transient expression vectors for GA733-Fc (A) and GA733-FcK
490   (B) proteins. GA733-Fc and GA733-FcK gene expression cassettes were introduced into the
491   pEAQ-*HT* plant transient expression vector. 35SP, Cauliflower mosaic virus 35S promoter; 5UTR,
492   Cowpea mosaic virus RNA-2 5′-UTR; 3UTR, Cowpea mosaic virus RNA-2 3′-UTR; P, suppressor
493   of gene silencing (P19); N Ⅱ, kanamycin resistance gene (NPT Ⅱ); K, endoplasmic reticulum
494   retention signal (KDEL); NOST, nopaline synthase gene terminator; 35ST, Cauliflower mosaic
495   virus 35S terminator. Expected protein structure of the recombinant fusion proteins GA733-Fc and
496   GA733-FcK: green oval-shaped bar, GA733; connected yellow bar, Fc domain; blue star-shaped
497   region, KDEL. Expected glycan structure: the symbols of the glycan structures are as follows: *N*-
498   acetylglucosamine, gray square; mannose, white circle; overlapped white diamonds, α(1,3)-
499   fucose; white triangle, β(1,2)-xylose.

500   **Figure 2.** Physical appearance of *N. benthamiana* leaves (top, middle, and base leaves) infiltrated
501   with Agrobacterial inoculum carrying pEAQ-GA733-Fc (Ag/pEAQ-GA733-Fc) (A) and pEAQ-
502   GA733-FcK (Ag/pEAQ-GA733-FcK) (B) for 1, 3, 5, 7, 8, 9, and 10 days post-infection (dpi). *N.*
503   *benthamiana* plants were grown for 4–5 weeks in a greenhouse at 24°C and 30% humidity, with
504   16 h light and 8 h dark. Six-week-old plants with similar number of leaves were used in this study.

505   **Figure 3.** PCR analysis of genomic DNA from plant leaves (top, middle, and base) at days
506   post infiltration (dpi) with Ag/pEAQ-GA733-Fc and Ag/pEAQ-GA733-FcK. Genomic DNA
507   was extracted from plant leaves expressing GA733-Fc (A) and GA733-FcK (B) according to
508   days post-infection (dpi) and leaf position (top, middle, and base leaves), and the targeted
509   genes were amplified and separated on a 1% agarose gel by electrophoresis. The 8–10 dpi
510   samples of base leaves for both GA733-Fc and GA733-FcK were insufficient for PCR. +:
511   positive control (GA733-Fc and GA733-FcK plasmid DNA extracted from *Escherichia coli*),
512   -: negative control (non-infiltrated plant): 1–10 days post-infiltration samples.

513   **Figure 4.** Comparison of expression levels at various times [1, 3, 5, 7, 8, 9, and 10 days post-
514   infiltration (dpi)] and leaf position (top, middle, and base) by western blot analysis (A), and
515   relative band intensity of GA733-Fc and GA733-FcK protein bands (~65kDa) with respect to
516   dpi (B). Western blot analysis was performed to identify GA733-Fc and GA733-FcK protein
517   expression levels in accordance with various dpi using agroinfiltrated leaves of *N.*
518   *benthamiana*. GA733-Fc and GA733-FcK were detected using murine anti-GA733 IgGs and

519   anti-murine IgG IgGs conjugated to horseradish peroxidase. +, positive control [mammalian-
520   derived GA733-Fc (GA733-Fc^M), 70 ng]; -, negative control (non-infiltrated plant); 1–10 dpi,
521   samples. (B) The graph shows relative band densities of GA733-Fc (W/O) and GA733-FcK
522   (W) proteins. The crude leaf extract was applied for western blot.

523   **Figure 5.** SDS-PAGE of purified GA733-Fc^P (W/O) and GA733-FcK^P (W) from infiltrated
524   leaves of *N. benthamiana* plants. The purified GA733-Fc^P and GA733-FcK^P were analyzed
525   by 10% SDS-PAGE. +, GA733-Fc^M (1 μg) as a positive control.

526   **Figure 6.** SDS-PAGE to confirm equal amounts of purified GA733-Fc^P and GA733-FcK^P proteins
527   and sandwich ELISA to assess binding activity of anti-GA733 antibody to both GA733-Fc^P and
528   GA733-FcK^P. Loading of the same quantity of GA733-Fc^P and GA733-FcK^P proteins in ELISA
529   was confirmed by SDS-PAGE (A). Schematic representation of the sandwich ELISA (B). Results
530   of ELISA for GA733-Fc^M, GA733-Fc^P, and GA733-FcK^P (C).

Figure 1

Schematic diagram of transient expression vectors for GA733-Fc (A) and GA733-FcK (B) proteins.

GA733-Fc and GA733-FcK gene expression cassettes were introduced into the pEAQ-*HT* plant transient expression vector. 35SP, Cauliflower mosaic virus 35S promoter; 5UTR, Cowpea mosaic virus RNA-2 5′-UTR; 3UTR, Cowpea mosaic virus RNA-2 3′-UTR; P, suppressor of gene silencing (P19); NII, kanamycin resistance gene (NPTII); K, endoplasmic reticulum retention signal (KDEL); NOST, nopaline synthase gene terminator; 35ST, Cauliflower mosaic virus 35S terminator. Expected protein structure of the recombinant fusion proteins GA733-Fc and GA733-FcK: green oval-shaped bar, GA733; connected yellow bar, Fc domain; blue star-shaped region, KDEL. Expected glycan structure: the symbols of the glycan structures are as follows: *N*-acetylglucosamine, gray square; mannose, white circle; overlapped white diamonds, α(1,3)-fucose; white triangle, β(1,2)-xylose.
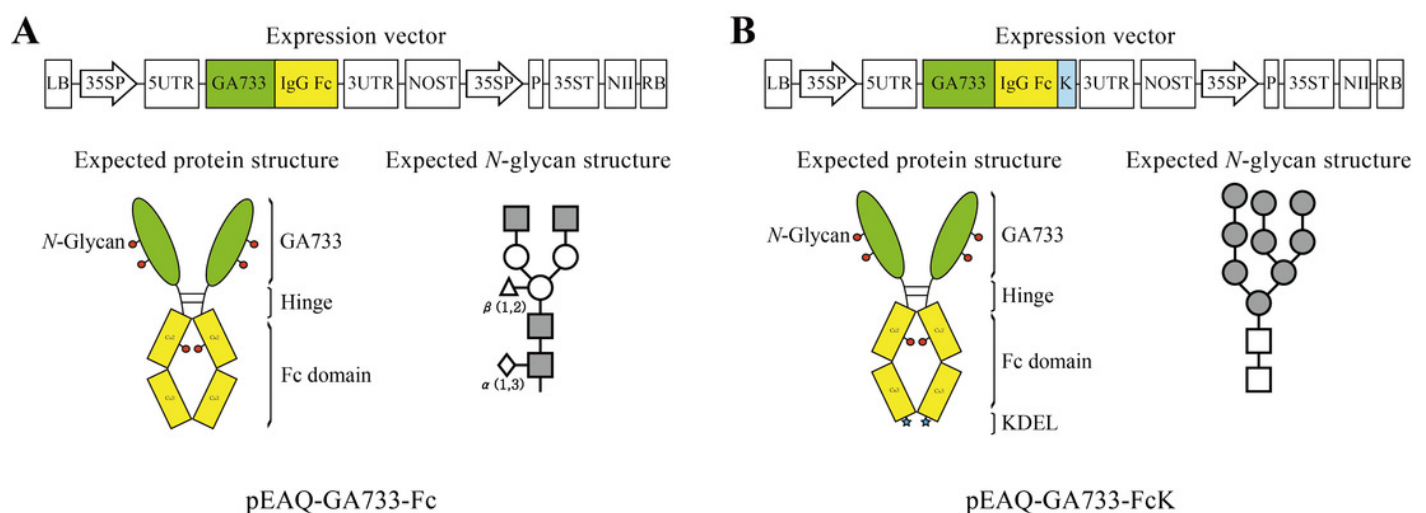
Figure 2

Physical appearance of *N. benthamiana* leaves (top, middle, and base leaves) infiltrated with Agrobacterial inoculum carrying pEAQ-GA733-Fc (Ag/pEAQ-GA733-Fc) (A) and pEAQ-GA733-FcK (Ag/pEAQ-GA733-FcK) (B) for 1, 3, 5, 7, 8, 9, and 10 days post-infec

N. benthamiana plants were grown for 4–5 weeks in a greenhouse at 24°C and 30% humidity, with 16 h light and 8 h dark. Six-week-old plants with similar number of leaves were used in this study.
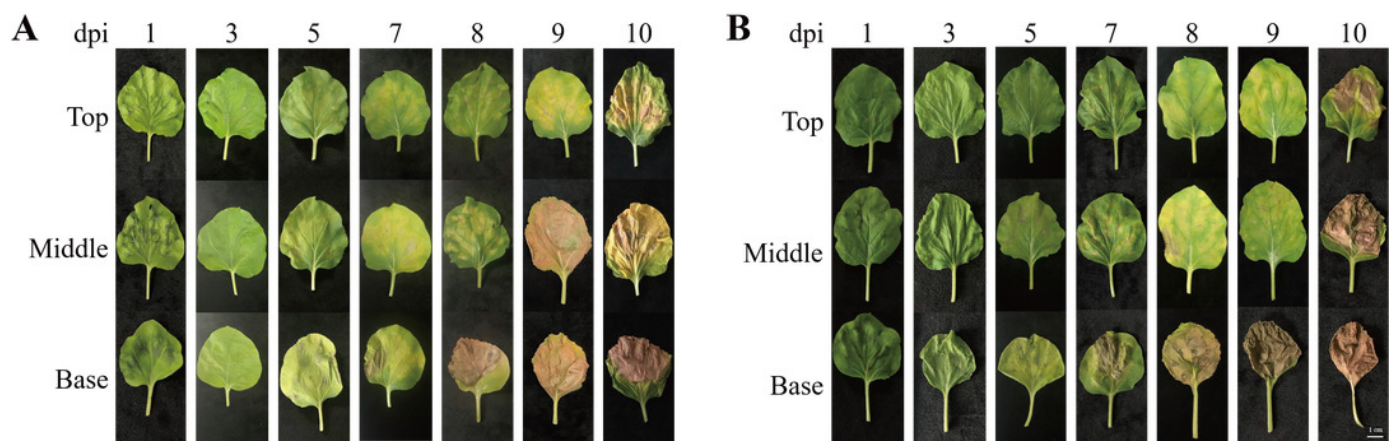
Figure 3

PCR analysis of genomic DNA from plant leaves (top, middle, and base) at days post infiltration (dpi) with Ag/pEAQ-GA733-Fc and Ag/pEAQ-GA733-FcK.

Genomic DNA was extracted from plant leaves expressing GA733-Fc (A) and GA733-FcK (B) according to days post-infection (dpi) and leaf position (top, middle, and base leaves), and the targeted genes were amplified and separated on a 1% agarose gel by electrophoresis. The 8–10 dpi samples of base leaves for both GA733-Fc and GA733-FcK were insufficient for PCR. +: positive control (GA733-Fc and GA733-FcK plasmid DNA extracted from *Escherichia coli*), -: negative control (non-infiltrated plant): 1–10 days post-infiltration samples.
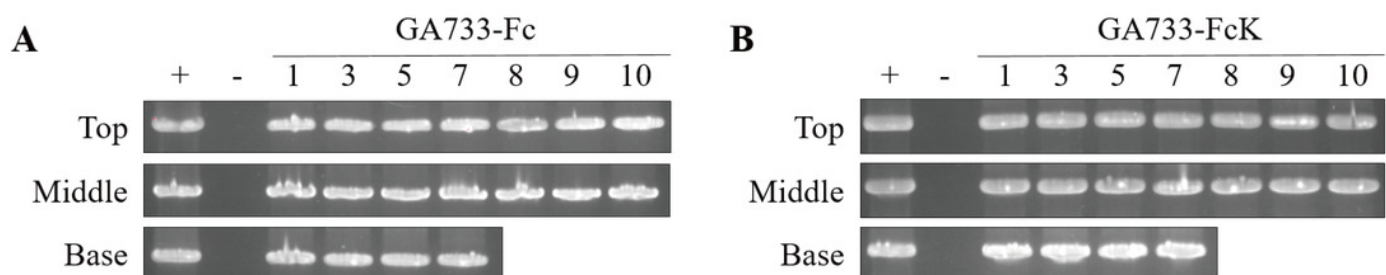
Figure 4

Comparison of expression levels at various times [1, 3, 5, 7, 8, 9, and 10 days post-infiltration (dpi)] and leaf position (top, middle, and base) by western blot analysis (A), and relative band intensity of GA733-Fc and GA733-FcK protein bands (~65kDa) w

Western blot analysis was performed to identify GA733-Fc and GA733-FcK protein expression levels in accordance with various dpi using agroinfiltrated leaves of *N. benthamiana*. GA733-Fc and GA733-FcK were detected using murine anti-GA733 IgGs and anti-murine IgG IgGs conjugated to horseradish peroxidase. +, positive control [mammalian-derived GA733-Fc (GA733-Fc^{M}), 70 ng]; -, negative control (non-infiltrated plant); 1–10 dpi, samples. (B) The graph shows relative band densities of GA733-Fc (W/O) and GA733-FcK (W) proteins. The crude leaf extract was applied for western blot.
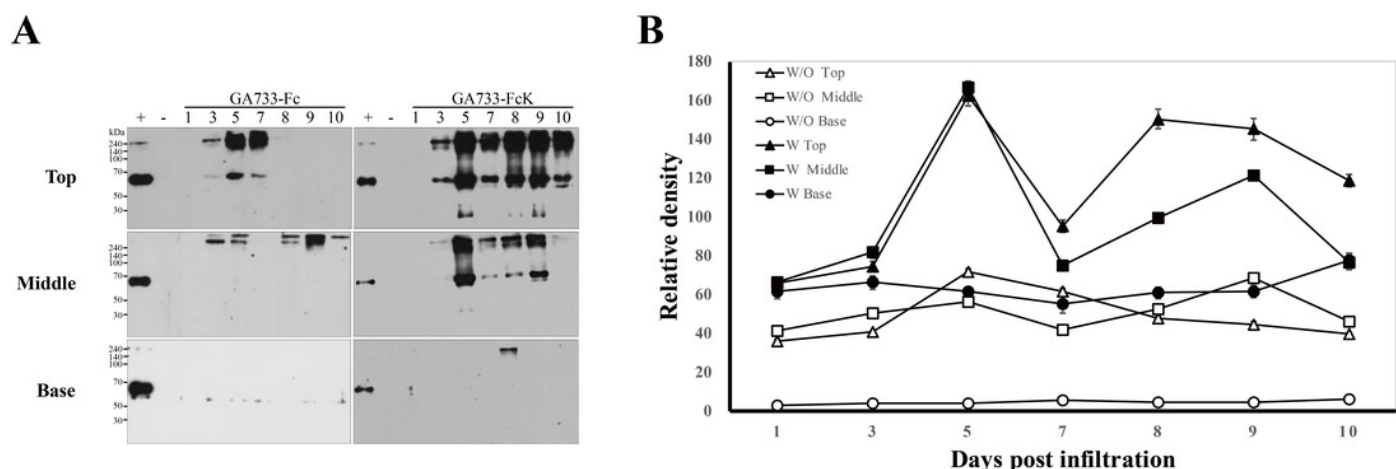
Figure 5

SDS-PAGE of purified GA733-Fc^P (W/O) and GA733-FcK^P (W) from infiltrated leaves of *N. benthamiana* plants.

The purified GA733-Fc^P and GA733-FcK^P were analyzed by 10% SDS-PAGE. +, GA733-Fc^M (1 μg) as a positive control.
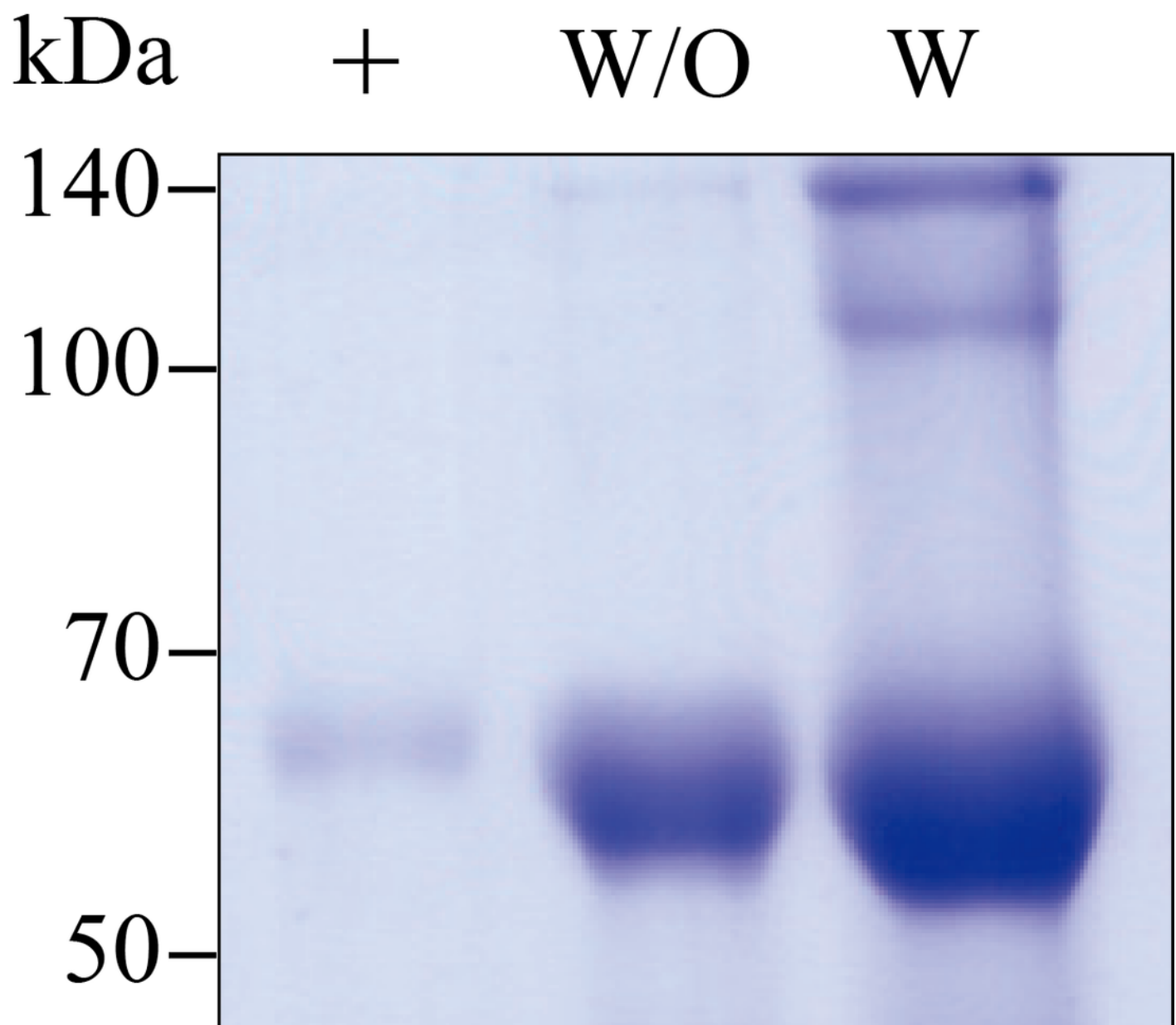
Figure 6

SDS-PAGE to confirm equal amounts of purified GA733-Fc^P and GA733-FcK^P proteins and sandwich ELISA to assess binding activity of anti-GA733 antibody to both GA733-Fc^P and GA733-FcK^P.

Loading of the same quantity of GA733-Fc^P and GA733-FcK^P proteins in ELISA was confirmed by SDS-PAGE (A). Schematic representation of the sandwich ELISA (B). Results of ELISA for GA733-Fc^M, GA733-Fc^P, and GA733-FcK^P (C).